Suppression and compensation effect of oxygen on the behavior of heavily boron-doped diamond films

Li-Cai Hao(郝礼才)[1], Zi-Ang Chen(陈子昂)[2,3], Dong-Yang Liu(刘东阳)[2,3], Wei-Kang Zhao(赵伟康)[2,3], Ming Zhang(张鸣)[2,3], Kun Tang(汤琨)[2,3,†], Shun-Ming Zhu(朱顺明)[2,3], Jian-Dong Ye(叶建东)[2,3], Rong Zhang(张荣)[2,3], You-Dou Zheng(郑有炓)[2,3], and Shu-Lin Gu(顾书林)[2,3,‡]

[1] *School of Integrated Circuits, Anhui University, Hefei* 230039, *China*

[2] *School of Electronic Science and Engineering, Nanjing University, Nanjing* 210093, *China*

[3] *Collaborative Innovation Center of Solid-State Lighting and Energy-Saving Electronics, Nanjing University, Nanjing* 210093, *China*

(Received 11 March 2022; revised manuscript received 10 June 2022; accepted manuscript online 8 July 2022)

This work investigates the suppression and compensation effect of oxygen on the behaviors and characteristics of heavily boron-doped microwave plasma chemical vapor deposition (MPCVD) diamond films. The suppression effect of oxygen on boron incorporation is observed by an improvement in crystal quality when oxygen is added during the diamond doping process. A relatively low hole concentration is expected and verified by Hall effect measurements due to the compensation effect of oxygen as a deep donor in diamond. A low acceptor concentration, high compensation donor concentration and relatively larger acceptor ionization energy are then induced by the incorporation of oxygen; however, a heavily boron-doped diamond film with high crystal quality can also be expected. The formation of an oxygen–boron complex structure instead of oxygen substitution, as indicated by the results of x-ray photoelectron spectroscopy, is suggested to be more responsible for the observed enhanced compensation effect due to its predicted low formation energy. Meanwhile, density functional theory calculations show that the boron–oxygen complex structure is easily formed in diamond with a formation energy of −0.83 eV. This work provides a comprehensive understanding of oxygen compensation in heavily boron-doped diamond.

Keywords: diamond, boron–oxygen co-doping, incorporation efficiency, ionization energy, compensation, boron–oxygen complex

PACS: 81.05.ug, 81.10.–h, 81.20.–n **DOI:** 10.1088/1674-1056/ac7f8a

1. Introduction

Boron-doped diamond is considered to be an excellent semiconductor with prospects for applications in heavy metal detection,[1,2] pH sensing[3,4] and electrochemical conversion.[5,6] Plasma chemical synthesis of boron-doped chemical vapor deposition (CVD) diamonds has attracted considerable attention due to its feasibility for synthesizing high-quality diamond and its convenience for controlling the doping concentration.[7] The properties of boron-doped diamond films have been widely investigated using the microwave plasma chemical vapor deposition (MPCVD) technique.[8–12] For example, Mortet *et al.*[12] reported that diamond with a high crystal quality was obtained by the MPCVD technique with a boron to carbon (B/C) ratio between 1000 ppm to 30000 ppm.

However, taking into account potential practical applications, diamond with a high crystal quality is crucial for achieving good performance of diamond-based devices.[13] Hence, much effort has been devoted to the synthesis of high-quality diamond by the MPCVD technique.[14,15] In recent years, co-doping technology has been frequently employed in the area of wide-bandgap semiconductor material growth, especially in diamond.[16–18] Co-doping is a promising strategy that can be used to effectively tune the dopant populations, electronic properties and magnetic properties, resulting in an increase in dopant solubility, an increase in the activation rate by lowering the ionization energy of acceptors and donors and an increase in the carrier mobility.[16] For example, the effect of co-doping of sulfur and boron on the crystal quality of diamond and their incorporation efficiency were studied by Liu *et al.*[17] They observed that sulfur incorporation led to evolution of the boron doping efficiency, hole mobility and concentration, crystal quality, surface morphology and growth rate. Boron and oxygen co-doped diamond has been prepared by MPCVD technology[19–23] and by ion implantation.[24,25] However, most of the previous literature has focused on the effect of oxygen on the diamond growth rate,[19] the crystal quality of diamond[20,21] and the boron incorporation efficiency[22,23] as well as the structural and electrical properties of diamond.[24,25] Works on the effect of oxygen on the active energy of boron and on the acceptor concentration, and the compensation effect of oxygen on boron-doped diamond, are quite rare. In particular, the compensation mechanism of oxygen is still not clear. We carried out the present work in order to obtain a comprehensive understanding of the

†Corresponding author. E-mail: ktang@nju.edu.cn

‡Corresponding author. E-mail: slgu@nju.edu.cn

© 2023 Chinese Physical Society and IOP Publishing Ltd

compensation mechanism of oxygen.

In this work, the suppression and compensation effects of oxygen on heavily boron-doped diamond films are fully investigated. The as-grown diamond films were characterized by atomic force microscopy (AFM), Fourier transform infrared spectroscopy (FTIR), optical emission spectroscopy (OES), Raman scattering spectroscopy, x-ray photoelectron spectroscopy (XPS) and Hall effect measurements. The effect of oxygen on the surface morphology, crystal quality, electronic properties and boron incorporation efficiency were systemically studied. What is more, the effect of oxygen on the ionization energy of boron acceptors and the compensation effect of oxygen on boron-doped diamond were also studied.

2. Experimental and theoretical calculation details

Diamond films were grown on (100)-oriented type Ib single-crystalline CVD diamond substrates (3.0 mm × 3.0 mm × 1.0 mm) by the MPCVD technique. Boron and oxygen were incorporated using diborane (B_2H_6) and oxygen (O_2) as the respective dopant gas sources. The molar ratio of the CH_4/H_2 mixture gas, growth pressure, substrate temperature and microwave power were 4%, 135 Torr, ∼ 850 °C and 3.8 kW, respectively. Boron-doped diamond films with different boron concentrations were grown with the boron to carbon ratio (B/C) fixed at 250 ppm, 1000 ppm, and 2500 ppm. To investigate the effect of oxygen on the properties of boron-doped diamond films, oxygen was added in the gas phase with the gas flow ratio of oxygen to carbon (O/C) kept at 0% (B/C = 2500 ppm), 2.5% (B/C = 2500 ppm), and 5.0% (B/C = 2500 ppm). Details on the operational processes and growth conditions can be found in the supplementary material. The surface morphology of diamond was obtained by AFM (NTEGRA) in tapping mode. Micro-Raman scattering spectra were recorded using a 514/633 nm laser as excitation with a confocal microscope (Horiba Jobin Yvon) at 100× magnification (numerical aperture, NA, 0.9). The electronic properties of diamond were measured on an HL5500PC Hall effect measurement system with a magnetic field of 0.6 T at variable temperatures from 300 K to 825 K. To achieve ohmic contacts, Ti (30 nm)/Au (100 nm) films were evaporation deposited and vacuum annealed at 500 °C for 0.5 h before the measurements. Details of the model for each apparatus and the specific conditions for each measurement can be found in the supplementary material.

The total energy and electronic structure of B–O defect complexes in diamond were studied through density functional theory based first-principles calculations. Our simulation uses a 2 × 2 × 2 supercell geometry containing 64 atoms. The valence–core interactions are described by the norm-conserving pseudopotentials, and the generalized gradient approximation (GGA) parameterized by Perdew, Burke and Ernzerhof (PBE) is employed for the exchange–correlation functional.[26,27] We adopt a plane-wave basis set with a cut-off energy of 340 eV. The total energy converges to 1×10^{-6} eV/atom for optimizing the electronic structure in the self-consistent calculation.[28,29] A 2 × 2 × 2 Monkhorst–Pack *k*-point mesh is adopted for integration in the first Brillouin zone.

3. Results and discussion

The surface morphology of boron-doped and boron and oxygen co-doped diamond films was characterized by AFM. As shown in Fig. 1, the surface of diamond films exhibits etching pits with the shape of an 'inverted pyramid'. A similar phenomenon had been observed by Fiori *et al.*,[30] and it was believed that the etching pits were related to the critical plasma chemistry. With increasing B/C gas flow ratio the density of the etching pits is increased, which indicates that the crystal quality of the diamond films decreases. This may be related to the lattice distortion induced by the incorporation of excess boron atoms. Moreover, with the incorporation of oxygen, the density of the etching pits is obviously decreased, and the root mean square (RMS) roughness decreases from 48.3 nm (O/C = 0%) to 9.7 nm (O/C = 2.5%), which suggests that the crystal quality has been improved.

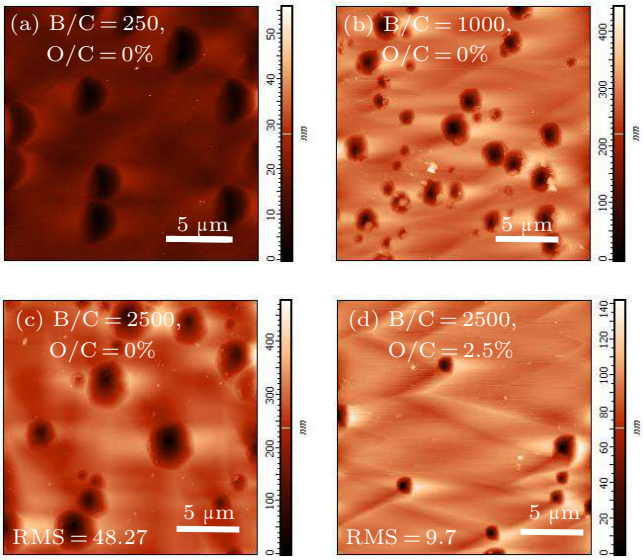


Fig. 1. AFM photographs of boron-doped and boron and oxygen co-doped diamond films: (a) B/C = 250 ppm, O/C = 0%; (b) B/C = 1000 ppm, O/C = 0%; (c) B/C = 2500 ppm, O/C = 0%; (d) B/C = 2500 ppm, O/C = 2.5%.

Raman scattering spectroscopy is a non-destructive technique widely used for the characterization of diamond. The full width at half maximum (FWHM) of the Raman peaks is representative of the crystal quality of diamond.[24] The Raman scattering spectra of boron-doped and boron and oxygen co-doped diamond films (with 514 nm excitation) are shown in Fig. 2(a). As shown in Fig. 2(a), the FWHM of the Raman

scattering peak of diamond films decreases from 2.86 cm^{-1} (O/C = 0%) to 2.69 cm^{-1} (O/C = 5.0%), which confirms that with the incorporation of oxygen the crystal quality of diamond has been improved. This may be related to the decrease in the growth rate of diamond with the incorporation of oxygen (as illustrated in Fig. 2(b)).

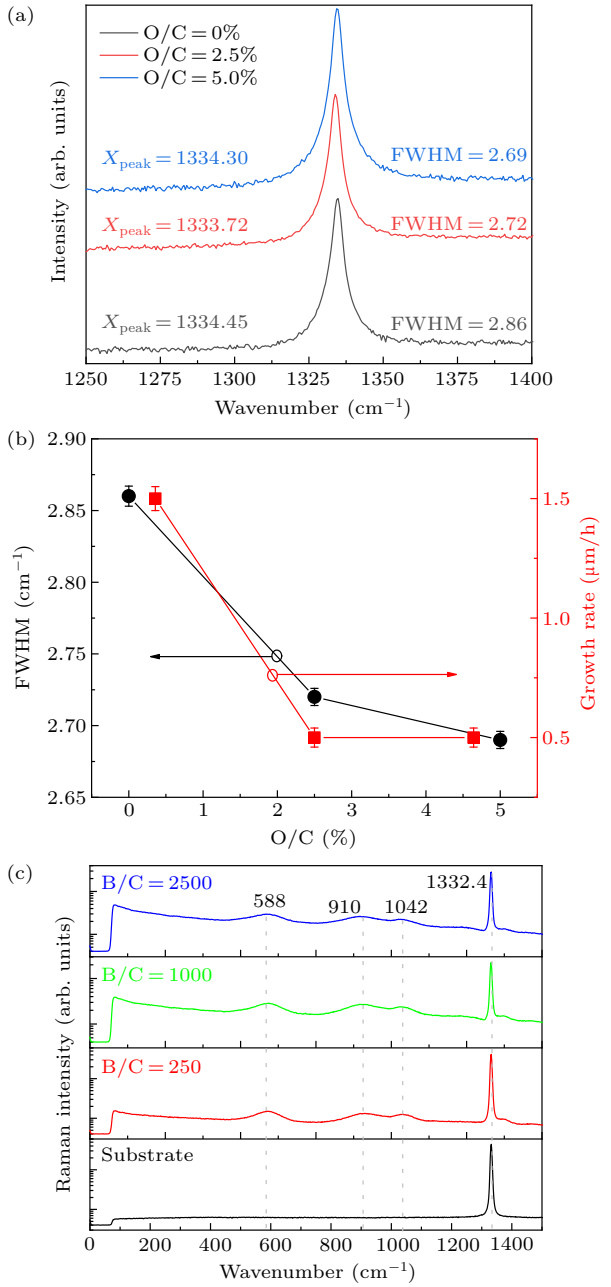


Fig. 2. (a) Raman scattering spectra of boron-doped and boron and oxygen co-doped diamond films with 514 nm excitation. (b) Growth rate of diamond films and the FWHM of the diamond Raman scattering peak as a function of the O/C ratio. (c) Raman scattering spectra of the CVD substrate and boron-doped diamond films with 633 nm excitation.

Figure 2(c) shows the Raman scattering spectroscopy of substrate and boron-doped diamond films (with a 633 nm excitation). As shown in Fig. 2(c), only an intense one-phonon diamond Raman line located at 1332.4 cm^{-1} was observed in the CVD substrate. With boron doping, the Raman scattering spectra exhibit an asymmetrical change and three new scattering peaks located at 588 cm^{-1}, 910 cm^{-1}, and 1024 cm^{-1} are observed. As described in the literature, the scattering peaks at 588 cm^{-1}, 910 cm^{-1}, and 1042 cm^{-1} may be related to the local mode vibration of boron atoms or the change in the diamond phonon density of states caused by defects.[31]

Hall effect measurements were performed at room temperature using an HL5500PC Hall effect measurement system. As shown in Fig. 3(a), with increasing B/C ratio the hole concentration increases from 8.1×10^{17} cm^{-3} (B/C = 250 ppm) to 5.7×10^{20} cm^{-3} (B/C = 1000 ppm) and then to 1.7×10^{21} cm^{-3} (B/C = 2500 ppm). Correspondingly, the hole mobility decreases from 11.7 $cm^2 \cdot V^{-1} \cdot s^{-1}$ (B/C = 250 ppm) to 0.4 $cm^2 \cdot V^{-1} \cdot s^{-1}$ (B/C = 1000 ppm) and then to 0.1 $cm^2 \cdot V^{-1} \cdot s^{-1}$ (B/C = 2500 ppm). These results show that more boron atoms were incorporated into diamond as the B/C ratio increased. The hole concentration increased to 10^{21} cm^{-3} when the B/C ratio was fixed at 2500 ppm, which indicates that the doping has reached a heavy doping level. With the incorporation of oxygen, however, as shown in Fig. 3(b), the hole concentration decreases from 1.7×10^{21} cm^{-3} (O/C = 0%) to 4.3×10^{19} cm^{-3} (O/C = 2.5%) and then to 1.5×10^{19} cm^{-3} (O/C = 5.0%), indicating that the boron concentration in diamond decreases with the incorporation of oxygen. In order to illustrate the effect of oxygen on the boron incorporation efficiency, the concentration of boron incorporated in diamond needs to be measured.

FTIR has proved to be a sensitive and powerful tool for characterizing the bond concentration in diamond.[32] Figure 3(c) illustrates the typical FTIR spectra of a CVD substrate and boron-doped and boron and oxygen co-doped diamond films. As shown in Fig. 3(c), three peaks located at 1970 cm^{-1}, 2030 cm^{-1}, and 2160 cm^{-1} are the characteristic peaks of diamond, which originate from the vibration of C–C bonds. With the incorporation of boron, a new peak located at 1290 cm^{-1} was observed, which has been correlated with boron content. The one-phonon absorption peak at 1290 cm^{-1} was used to calculate boron concentration with the formula[32]

$$B\left(\mathrm{cm}^{-3}\right) = 2.1 \times 10^{17} \times \alpha\left(\text{at } 1290\,\mathrm{cm}^{-1}\right), \quad (1)$$

$$\alpha\left(\text{at } 1290\,\mathrm{cm}^{-1}\right) = \frac{A\left(\text{at } 1290\,\mathrm{cm}^{-1}\right)}{t}, \quad (2)$$

where B and t are the boron concentration in diamond and the film thickness, respectively. A is the integrated intensity of the absorbance from 1250 cm^{-1} to 1300 cm^{-1}. The calculated boron concentrations in diamond are 6.4×10^{21} cm^{-3} (O/C = 0%), 8.7×10^{20} cm^{-3} (O/C = 2.5%), and 9.3×10^{19} cm^{-3} (O/C = 5.0%), respectively. The boron concentration decreased with incorporation of oxygen (as shown in Fig. 3(d)), which shows that oxygen decreases the incorporation efficiency of boron.

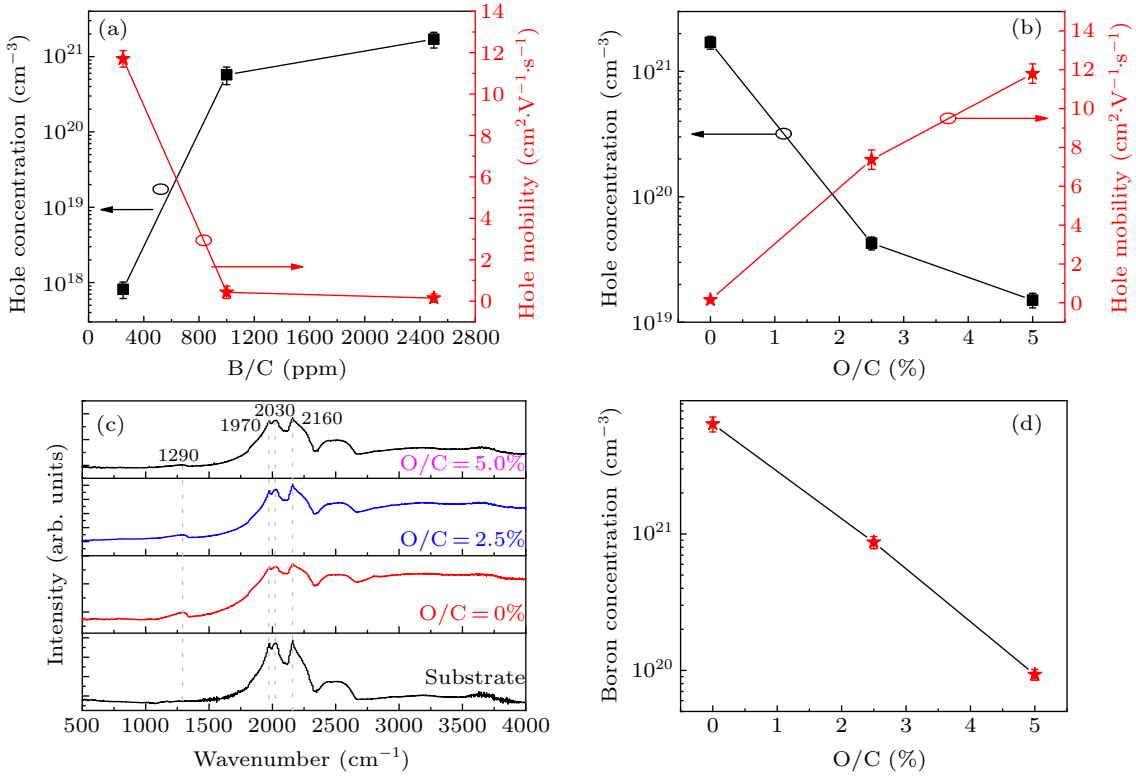


Fig. 3. (a) Hole concentration and hole mobility of boron-doped diamond as a function of the B/C ratio. (b) Hole concentration and hole mobility of boron-doped and boron and oxygen co-doped diamond as a function of the O/C ratio. (c) FTIR spectra of the CVD substrate and boron-doped and boron and oxygen co-doped diamond films. (d) The calculated boron concentration in diamond.

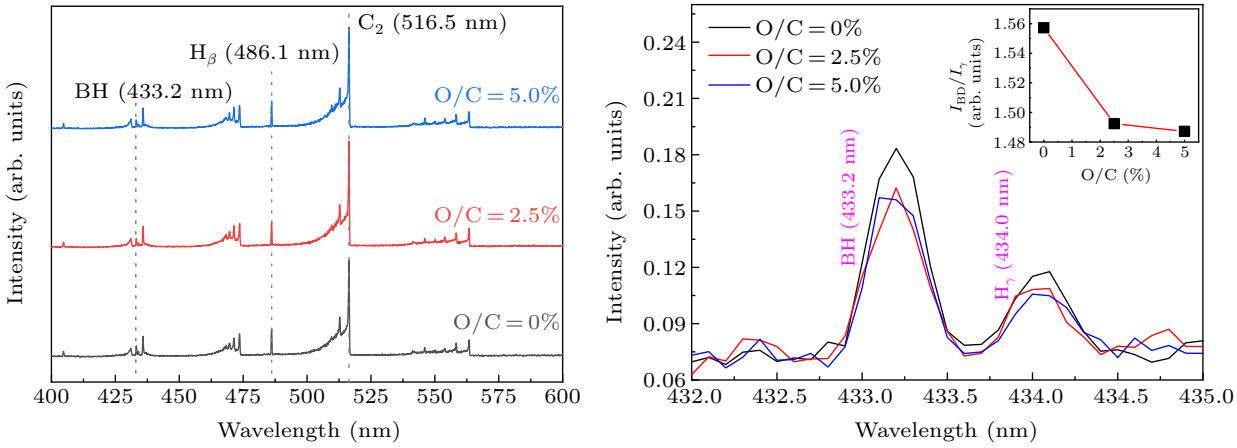


Fig. 4. (a) OES results for CH_4–H_2–B_2H_6 and CH_4–H_2–B_2H_6–O_2 mixtures in the MPCVD system. (b) Enlarged view of the OES spectra with wavelengths from 432 nm to 435 nm. The inset shows the intensity ratio of BH radicals to atomic hydrogen H_γ radicals as a function of the O/C ratio.

In order to further illustrate the effect of oxygen on the incorporation efficiency of boron, OES was employed to analyze the composition of the gas mixture. Figure 4 shows the OES results for CH_4–H_2–B_2H_6 and CH_4–H_2–B_2H_6–O_2 mixtures in the MPCVD system. As shown in Fig. 4(a), the optical emission lines located at 434.0 nm and 486.1 nm originate from atomic hydrogen H_γ radicals and atomic H_β radicals,[33] respectively. The optical emission lines located at 433.2 nm and 516.6 nm originate from BH and C_2 radicals,[34] respectively. As illustrated in Fig. 4(b), the intensity ratio of BH radicals to atomic hydrogen H_γ radicals decreases with increase in the O/C ratio, which indicates that the boron incorporation efficiency has decreased. Hence, the FTIR and OES results confirm that oxygen decreases the incorporation efficiency of boron in diamond.

In order to investigate the influence of oxygen on the ionization energy of boron, the as-grown diamond films were investigated by Hall effect measurements with measurement temperatures from 300 K to 825 K. Figure 5(a) shows that the resistivity of boron-doped and boron and oxygen co-doped diamond films varies with measurement temperatures from 300 K to 825 K. As illustrated in Fig. 5(a), the resistivity of diamond decreases with increasing temperature. What is more, literature reports state that the ionization energy of boron ac-

ceptors can be fitted to the temperature dependence of the resistivity by the following formula:[35]

$$\ln\rho = \ln A - \frac{E_a}{k_B}\cdot\frac{1}{T}. \tag{3}$$

In formula (3), ρ ($\Omega\cdot$cm) and E_a (eV) represent the resistivity of diamond and the ionization energy of the boron acceptor, respectively. k_B is the Boltzmann constant. The fitted graphs are shown in Figs. 5(b)–5(d) and the fitted ionization energy of boron acceptors is 43.4 meV. The fitted ionization energies of boron and oxygen co-doped diamond are 56.8 meV (O/C = 2.5%) and 71.8 meV (O/C = 5.0%), respectively. These results show that the ionization energy of boron acceptors increases with the incorporation of oxygen. This may be related to a decrease in the boron concentration in diamond induced by oxygen (the FTIR results confirm that the concentration of boron in diamond decreases with the incorporation of oxygen).

For a p-type semiconductor, the general description of the hole concentration p at a temperature T is given by the following equation:[36]

$$\frac{g_d p\,(N_D + p)}{M_V\,(N_A - N_D - p)} = \exp\left(-\frac{E_i}{k_B T}\right). \tag{4}$$

Here, E_i and k_B are the ionization energy of the acceptor and the Boltzmann constant, respectively. N_A and N_D are the acceptor concentration and donor concentration, respectively. M_V and p are the effective density of states of the valence band and the hole concentration in diamond, respectively. g_d is the acceptor degeneracy. The acceptor concentration and donor concentration were fitted by MATLAB 9.0 with a curve fitting package tool (the fitting curve is shown in Fig. S1). For boron-doped diamond, the fitted acceptor concentration (N_A) and donor concentration (N_D) are 2.6×10^{21} cm^{-3} (O/C = 0%) and 6.6×10^{16} cm^{-3} (O/C = 0%), respectively. The donor concentration originates from unintentionally doped nitrogen atoms during the preparation of the film. For boron and oxygen co-doped diamond, the fitted acceptor concentrations (N_A) are 1.8×10^{20} cm^{-3} (O/C = 2.5%) and 5.0×10^{19} cm^{-3} (O/C = 5.0%). The corresponding fitted donor concentrations (N_D) are 7.9×10^{17} cm^{-3} (O/C = 2.5%) and 1.7×10^{18} cm^{-3} (O/C = 5.0%). The results show that, with increasing O/C ratio, the acceptor concentration (N_A) decreases and the donor concentration (N_D) increases. Our analysis is that as oxygen as a donor exits the diamond oxygen compensation is increased with increasing O/C ratio, which results in a decrease in the acceptor concentration (N_A).

In order to evaluate the effect of the oxygen compensation mechanism on boron doping behavior, the XPS spectra were analyzed. Figure 6 shows the carbon, boron and oxygen 1s core level XPS signals of boron and oxygen co-doped diamonds. For the carbon 1s line, four peaks have been deconvoluted, and the 283.1 eV peak and 286.0 eV peak are assigned to the C–B bond and C–O bond,[37] respectively. The 283.8 eV

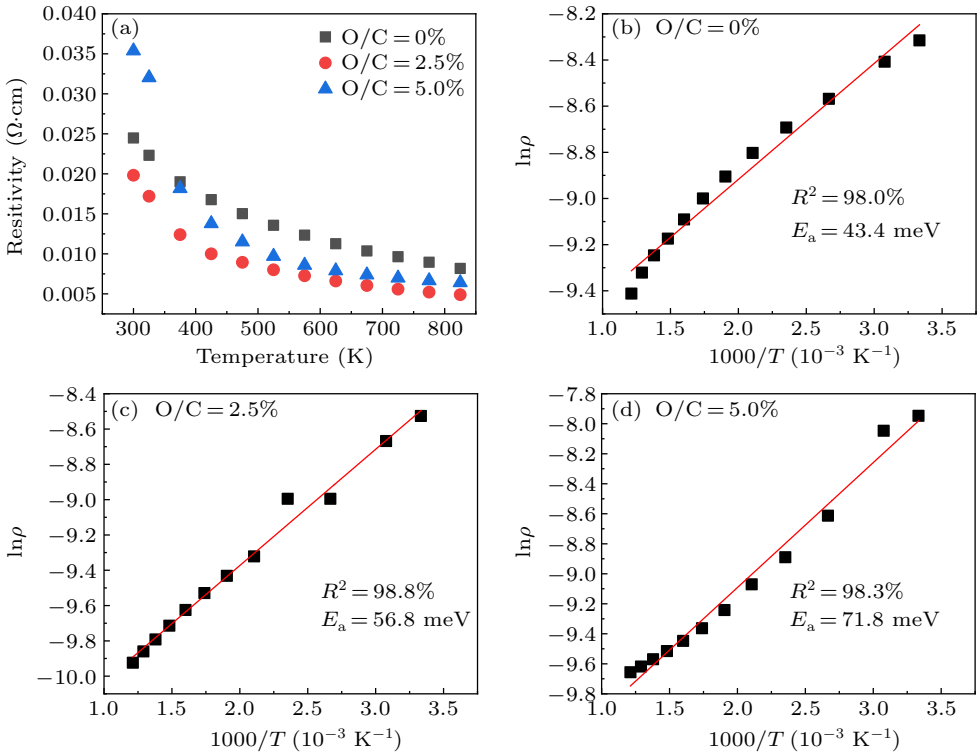


Fig. 5. (a) Resistivity of boron-doped and boron and oxygen co-doped diamond films as a function of temperature. (b) Fitting of the activation energy of boron-doped (O/C = 0%) diamond by the relation between resistivity and temperature. (c) Fitting of the activation energy of boron and oxygen co-doped (O/C = 2.5%) diamond by the relation between resistivity and temperature. (d) Fitting of the activation energy of boron and oxygen co-doped (O/C = 5.0%) diamond by the relation between resistivity and temperature.

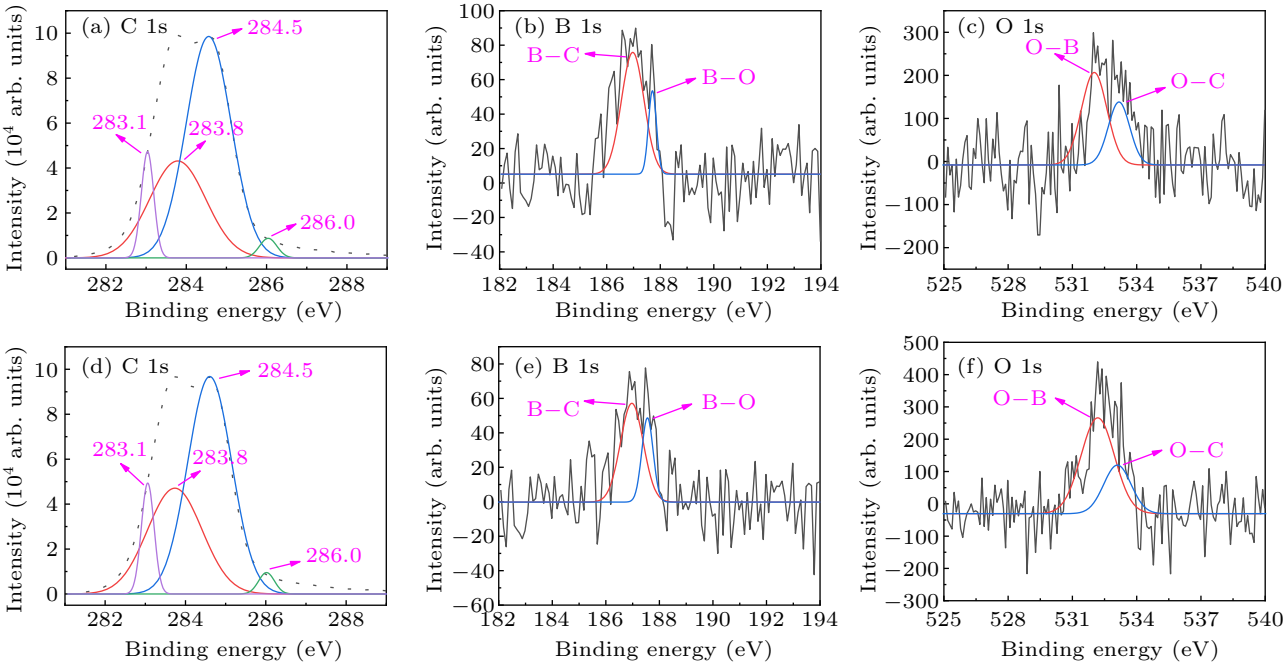


Fig. 6. (a)–(c) Carbon 1s, boron 1s and oxygen 1s XPS spectra of boron and oxygen co-doped (O/C = 2.5%) diamond. (d)–(f) Carbon 1s, boron 1s and oxygen 1s XPS spectra of boron and oxygen co-doped (O/C = 5.0%) diamond.

peak and 284.5 eV peak are ascribed to the C–C bond (sp^2) and C–C bond (sp^3),[37] respectively. Two peaks of the boron 1s lines originate from the B–C (187.0 eV) and B–O (187.7 eV) bonds.[38] Two peaks of oxygen 1s lines are ascribed to the O–B (532.1 eV) and O–C (533.0 eV) bonds.[38] Moreover, XPS is also known as a powerful tool for quantifying the doping concentration of the dopants by comparing the relative area ratio among components by considering the sensitivity factor of each component.[37] In order to illustrate the relative doping concentration of boron, we determined the area ratio of boron 1s lines over the sum of the area of carbon 1s, boron 1s and oxygen 1s lines (the oxygen doping concentration is also calculated as boron). As shown in Fig. 6, with increasing O/C ratio from 2.5% to 5.0%, the boron component in diamond decreases from 0.091% to 0.073% and the oxygen component in diamond increases from 0.042% to 0.052%, which implies that with increasing O/C ratio more oxygen atoms are incorporated into diamond. Hence, oxygen compensation is increased and the acceptor concentration (N_A) is decreased.

Furthermore, for the oxygen 1s line we determined the ratio of the O–B component to the O–B and O–C components. It was interesting to find that the O–B component in diamond increases from 63.49% to 73.73%. At the same time, for the boron 1s line, we determined the ratio of the B–O component to the B–O and B–C components in the boron 1s line. The results show that the B–O component in diamond increases from 19.35% (O/C = 2.5%) to 29.88% (O/C = 5.0%), which is consistent with the result derived from the oxygen 1s line. These results show that with the introduction of oxygen into boron-doped diamond, a B–O complex structure is easily formed in diamond, with a level of 0.574 eV below the conduction band. In order to check the stability of the B–O complex, we carried out brief first-principles density functional theory calculations on the diamond lattice with a B–O complex structure.

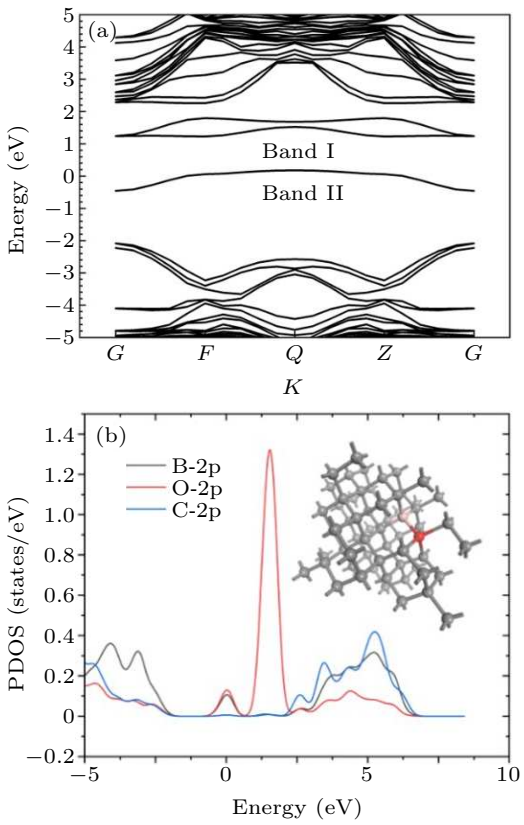


Fig. 7. (a) The band structure and (b) the partial density of states (PDOS) of a B–O complex in a diamond lattice. The inset in (b) shows the structure of the B–O complex in a diamond host lattice.

We built a 64-atom $2 \times 2 \times 2$ supercell with a B–O com-

plex in the diamond host lattice. Firstly, the formation energy of the B–O complex in diamond was only −0.83 eV, suggesting that the complex structure is quite stable in a diamond lattice. Secondly, figure 7 shows both the band structure and the partial density of states of the diamond lattice with a B–O complex. Two extra bands are observed in the forbidden band. After comparing the energy level between Figs. 7(a) and 7(b), band I is attributed to a deep level almost solely related to the oxygen 2p orbital, whereas band II originates from the hybridization of the B 2p and O 2p orbitals. Both extra energy bands are quite deep and could act as compensation centers for the shallow boron acceptors.

4. Summary

In conclusion, the suppression and compensation behaviors of oxygen in heavily boron-doped diamond films were systematically investigated. With incorporation of oxygen, the crystal quality of diamond is improved and the oxygen decreases the boron incorporation efficiency. Moreover, the ionization energy of boron is increased, and the acceptor concentration is decreased with oxygen incorporation, which is related to the fact that oxygen exists as a donor in diamond so the co-doping of oxygen would compensate the boron acceptor. What is more, with incorporation of oxygen, a B–O complex structure is formed. Density functional theory calculations show that the B–O complex structure is easily formed in diamond with a formation energy of −0.83 eV.

Acknowledgments

Project supported by the National Key Research and Development Program of China (Grant Nos. 2018YFB0406502, 2017YFF0210800, and 2017YFB0403003), the National Natural Science Foundation of China (Grant Nos. 61774081, 61775203, 61574075, 61974059, 61674077, 61774081, and 91850112), the State Key Research and Development Project of Jiangsu, China (Grant No. BE2018115), State Key Laboratory of Wide-Bandgap Semiconductor Power Electric Devices (Grant No. 2017KF001), and Anhui University Natural Science Research Project (Grant No. KJ2021A0037).

References

[1] Guo C Y, Zheng J G, Deng H W, Shi P H and Zhao G H 2021 *Carbon* **175** 454
[2] Liu T, Yang X G, Li Z, Hu Y W, Lv C F, Zhao W B, Zang J H and Shan C X 2020 *Chin. Phys. B* **29** 108102
[3] Zhang T T, Pramanik G, Zhang K, Gulka M, Wang L Z, Jing J X, Xu F, Li Z F, Wei Q, Cigler P and Chu Z Q 2021 *ACS Sens.* **6** 2077
[4] Wang S H, Wang T and Tang Y B 2021 *Small* **17** 2007529
[5] Yu S Y, Yang N J, Liu S T and Jiang X 2021 *Carbon* **175** 440
[6] HU X J and Li N 2013 *Chin. Phys. Lett.* **30** 088102
[7] Ren Z Y, Zhang J F, Zhang J C, Xu S R, Zhang C F, Su K, Li Y and Hao Y 2018 *Chin. Phys. Lett.* **35** 078101
[8] Sheng L X, Chen C K, Jiang M Y, Li X and Hu X J 2020 *Chin. Phys. B* **29** 088101
[9] Yang B, Li H N, Yu B, Lu J Q, Huang N, Liu L S and Jiang X 2021 *Carbon* **171** 455
[10] Li H D, Zou G T, Wang Q L, Cheng S H, Li B, Lv J N, Lv Z Y and Jin Z S 2008 *Chin. Phys. Lett.* **25** 1803
[11] Wang Q L, Lv X Y, Li L A, Cheng S H and Li H D 2010 *Chin. Phys. Lett.* **27** 047802
[12] Mortet V, Živcová Z V, Taylor A, Davydová M, Frank O, Hubík P, Lorincik J and Aleshin M 2019 *Diam. Relat. Mater.* **93** 54
[13] Yang M C, Wan L F, Wang J C, Ma Z C, Wang P, Gao N and Li H D 2020 *Chin. Phys. Lett.* **37** 066801
[14] Kubo Y, Temgoua S, Issaoui R, Barjon J and Naka N 2019 *Appl. Phys. Lett.* **114** 132104
[15] Soleimanzadeh R, Naamoun M, Floriduz A, Khadar R A, Erp R V and Matioli E 2021 *ACS Appl. Mater. Interfaces* **13** 43516
[16] Imanishi S, Kudara K, Ishiwata H, Horikawa K, Amano S, Iwatak M, Morishita A, Hiraiwa A and Kawarada H 2020 *IEEE Electr. Device L.* **42** 204
[17] Liu D Y, Hao L C, Chen Z A, Zhao W K, Shen Y, Bian Y, Tang K, Ye J D, Zhu S M, Zhang R, Zheng Y D and Gu S L 2020 *Appl. Phys. Lett.* **117** 022101
[18] Hao L C, Shen Y, Yang X D, Bian Y, Du Q Q, Liu D Y, Zhao W K, Ye J D, Tang K, Wu H P, Zhang R, Zheng Y D and Gu S L 2020 *J. Phys. D: Appl. Phys.* **53** 075107
[19] Issaoui R, Achard J, William L, Thaury M A P and Benedic F 2019 *Diam. Relat. Mater.* **94** 88
[20] Issaoui R, Achard J, Silva F, Tallaire A, Mille V and Gicquel A 2011 *Phys. Status Solidi A* **208** 2023
[21] Achard J, Issaoui R, Tellier A, F. Silva1, Barjon J, Jomard F and Gicquel A 2012 *Phys. Status Solidi A* **209** 1651
[22] Volpe P N, Arnault J C, Tranchant N, Chicot G, Pernot J, Jomard F and Bergonzo P 2012 *Diam. Relat. Mater.* **22** 136
[23] Bogdanov S A, Vikharev A L, Drozdov M N and Radishev D B 2017 *Diam. Relat. Mater.* **74** 59
[24] Hu X J, Shen Y G, Hao X P and Wang B Y 2009 *Diam. Relat. Mater.* **18** 210
[25] Hu X J, Ye J S, Liu H J, Hu H and Chen X H 2011 *Diam. Relat. Mater.* **20** 246
[26] Kresse G and Furthmuller J 1996 *Phys. Rev. B* **54** 11169
[27] Perdew J P, Burke K and Ernzerhof M 1996 *Phys. Rev. Lett.* **77** 3865
[28] Grimme S 2006 *J. Comput. Chem.* **27** 1787
[29] Kresse G and Joubert D 1999 *Phys. Rev. B* **59** 1758
[30] Fiori A and Teraji T 2017 *Diam. Relat. Mater.* **76** 38
[31] Blank V D, Denisov V N, Kirichenko A N, Kuznetsov M S, Mavrin B N, Nosukhin S A and Terentiev S A 2008 *Diam. Relat. Mater.* **17** 1840
[32] Karna S K, Martyshkin D V, Vohra Y K and Weir S T 2013 *MRS Online Proceedings Library* 1519
[33] Zhou Z Y, Chen G C, Tang W Z and Lv F X 2006 *Chin. Phys.* **15** 1009
[34] Vandeveldea T, Wu T D, Quaeyhaegens C, Vlekken J, DOlieslaeger M and Stals L 1999 *Thin Solid Films* **340** 159
[35] Nicley S S 2015 *The boron doping of single crystal diamond for high power diode applications* (ProQuest Dissertations Publishing)
[36] Barjon J, Chikoidze E, Jomard F, Dumont Y, Pinault-Thaury M A, Issaoui R, Brinza O, Achard J and Silva F 2012 *Phys. Status Solid A* **209** 1750
[37] Rossi K L, Budzinski R C, Boaretto B R R, Prado T L, Feude U and Lopes S R 2021 *Chaos* **31** 083121
[38] Liu X B, Chen X, Singh D J, Stern R A, Wu J S, Petigirard S, Bina C R and Jacobsen S D 2019 *Proc. Natl. Acad. Sci. USA* **116** 7703